A Pacific Aerosol Survey. Part I: A Decade of Data on Particle Production, Transport, Evolution, and Mixing in the Troposphere*

ANTONY D. CLARKE AND VLADIMIR N. KAPUSTIN

University of Hawaii, Honolulu, Hawaii

(Manuscript received 29 December 2000, in final form 27 July 2001)

ABSTRACT

Integration of extensive aerosol data collected during the past decade around the Pacific basin provides a preliminary assessment of aerosol microphysics for this region and cycling of aerosol in the troposphere. These include aircraft-based data collected as part of numerous field experiments supported by the National Aeronautics and Space Administration (NASA), the National Science Foundation (NSF), and the National Oceanic and Atmospheric Administration (NOAA) [Global Backscatter Experiment (GLOBE), First Aerosol Characterization Experiment (ACE-1), Pacific Exploratory Mission (PEM)-Tropics A and B]. Although these experiments had diverse goals, most included extensive data on aerosol size distributions, optical properties (light scattering and light absorption), and chemistry. Vertical profiles of aerosol concentration, size distribution, and light scattering were used to characterize vertical structure from 70°S to 70°N. The in situ data are placed in the context of meteorological regimes over the Pacific as well as processes associated with particle formation, growth, and evolution, and include dust, pollution, sea salt, sulfates, and clean cloud–processed air. The Tropics commonly have low aerosol mass but very high number concentrations in the upper free troposphere (FT) that appear to form from sulfuric acid (nucleation) in convective regions and near cloud edges. These age and subside to become effective cloud condensation nuclei (CCN) when mixed into the marine boundary layer. Fewer number but larger aerosol are more evident in the midlatitude FT. These can often be internally mixed and with a nonvolatile core indicative of black carbon with volatile components (sulfate, organics, etc.). In the North Pacific springtime a combustion-derived aerosol is frequently found associated with the same meteorology that transports ''dust events.'' Both constituents may dominate the scattering and absorption properties of the aerosol even though the increase in large dust particles in such events generally dominates the mass. The FT in the subtropics tends to exhibit frequent and marked transitions and mixing between these clean and continental aerosol types.

1. Introduction

Assessment of global aerosol fields and their variability in space and time will unquestionably require effective interpretation of remotely sensed data from satellites. However, the variations in aerosol and other parameters that influence satellite-derived radiance introduce significant uncertainty into the inversions needed for the retrieval of aerosol properties. Consequently, in situ measurements of column aerosol properties are required to confirm inferred aerosol fields and related radiation fields. The aerosol size distribution needs to be known over a range that can adequately describe the mass, surface area, and number of aerosol types that can impact the issues related to both climate and global transport. The aerosol *direct* radiative effect (Charlson et al. 1992) is most closely linked to aerosol surface area for diameters D_p between about 0.1 μm $< D_p <$ 10 μm, since these sizes best describe the interaction of aerosol in the scattering of light. The *indirect* effect (Charlson et al. 1987) of aerosol is more closely linked to aerosol number for 0.05 μm $< D_p <$ 1 μm since these particle sizes typically dominate the cloud condensation nuclei (CCN) spectra. Because most emission source characterizations have been made on a basis of aerosol mass it is also essential to have an understanding of the relationship of particle mass and composition (e.g., sulfate, black carbon, organics, dust, sea salt) to particle surface area and number in order to identify the contributions of specific aerosol types to either *direct* or *indirect* effects.

Global assessments, satellite interpretation, and process studies all require improved understanding of vertical profiles of aerosol and links between the marine boundary layer (MBL) and the free troposphere (FT). Much of the progress in MBL aerosol characterization came recently through extensive cruises in the 1980s and 1990s and has been the subject of numerous reviews

* School of Ocean and Earth Science and Technology Contribution Number 5870.

Corresponding author address: Antony D. Clarke, Department of Oceanography, University of Hawaii, 1000 Pope Road, MSB205, Honolulu, HI 96822.
E-mail: tclarke@soest.hawaii.edu

focusing on surface data suggestive of global distributions of number concentration, and more recently on size distributions (Hoppel et al. 1990; Clarke 1993; Fitzgerald 1991; Quinn et al. 1995, 1996; O'Dowd et al. 1997; Heintzenberg et al. 2000). Surface measurements have revealed a general picture of low number concentrations in the central parts of the oceans and increasing values toward the downwind coast of the continents, but processes that maintain these concentrations remain unclear.

However, it is clear that MBL aerosol and FT aerosol are coupled through mixing and entrainment (Clarke and Porter 1993; Clarke et al. 1996; Covert et al. 1996; Clarke et al. 1997; Solazzo et al. 2000; Clarke et al. 2001, hereafter C01). Moreover, case studies have revealed natural sources of aerosol production aloft (Clarke et al. 1999a,b) consistent with model results (Raes et al. 1995) as well as numerous cases of plumes undergoing long-range transport (C01; Browell et al. 2001, manuscript submitted to *J. Geophys. Res.*; Moore et al. 2000, manuscript submitted to *J. Geophys. Res.*; Staudt et al. 2001, manuscript submitted to *J. Geophys.*). These observations undermine the notion of ''a global background aerosol.'' Instead, a dynamic system of independent sources and sinks exists that tends to result in aerosol ''rivers,'' ''layers,'' and ''regions'' in the troposphere with specific microphysical and chemical characteristics. However, as these data suggest, there is evidence for gas phase production processes that result in a ''natural'' aerosol source on global scales upon which continental perturbations are superimposed.

A global-scale aerosol climatology is needed for model testing, satellite validation observations, and for any quantitative regional or global assessment of aerosol effects on the earth's system (Stowe et al. 1997). Recently launched satellites promise to provide improved information on aerosol properties through selection of more and narrower wavelength bands, multiple view angles, higher resolution, etc. (e.g., moderate-resolution imaging spectroradiometer, multiangle imaging spectrometer, Cloud and the Earth's Radiant Energy System; King et al. 1999). Such data has added value if it can be related to processes that govern the source, transformation, and removal of aerosol in the atmosphere. The development of an observation-derived aerosol climatology appropriate to column properties and related to satellite assessment of *direct* or *indirect* forcing requires a combination of surface and aircraft in situ measurements. The data are particularly desirable over remote oceanic regions where satellite measurements (e.g., Advanced Very High Resolution Radiometer) have the best opportunity for assessing aerosol fields. Such data are typically expensive to acquire and hard to obtain even for limited validation programs.

Here we assemble and interpret what is arguably one the most extensive and complete datasets available on FT aerosol size and properties throughout the North and South Pacific that were collected as part of our previous aircraft campaigns (Fig. 1). These datasets are being combined here in order to establish aerosol characteristics and regimes that can be used to build a Pacific aerosol climatology of value to addressing *direct* and *indirect* forcing. Although these datasets were collected for diverse objectives, all include well-resolved particle size distributions, condensation nuclei (CN) concentrations and most include size-resolved aerosol composition (thermally determined), aerosol light-scattering (nephelometer), aerosol light absorption [particle soot absorption photometer (PSAP)]. These measurements span at least five meteorological zones of global significance over the North and South Pacific and include transects aloft in the FT, boundary layer runs, and 270 vertical profiles.

Here we examine data that we believe can provide constraints on the range of possibilities and guide the interpretation of global scale models. Even so, the vast horizontal and vertical extent of these Pacific regions challenges the ability of aircraft missions to adequately represent all of their features either spatially or temporally. Hence, we do not attempt to provide 3D statistics for our measurements over some 3D gridded array since grid averages would either not exist or not be robust in most cases. However, some statistical evaluation of the mean latitudinal and vertical data over selected regional ranges has been included to illustrate major features.

2. Aerosol data collection

a. Aircraft experiments over the Pacific

Figure 1 shows a map of our aircraft missions over the Pacific during the past decade. Vertical profiles and column integrated aerosol data are available for all flight leg endpoints and for numerous locations along the flight legs. Aircraft data can provide the critical vertical information required for satellite column comparisons and data on aerosol fields aloft in the FT. However, flights are generally limited to about 8 h and seldom for consecutive days or similar regions so that continuity and time series are hard to achieve. Even so, the rapid coverage of extended regions and numerous vertical profiles provides a substantial survey and a valuable tool for interpreting satellite and model data for a wide variety of aerosol types and regimes. In many cases the column-averaged size distributions can describe the key aerosol optical properties needed to constrain and test satellite retrieval algorithms. Missions flown include the following.

The Global Backscatter Experiment (GLOBE-2, 1990) was designed to characterize the spatial, temporal, and spectral variability of atmospheric aerosol lidar backscatter coefficients in the Pacific troposphere measured from the National Aeronautics and Space Administration (NASA) DC-8 aircraft. Aerosol physiochemical measurements were also made over a broad

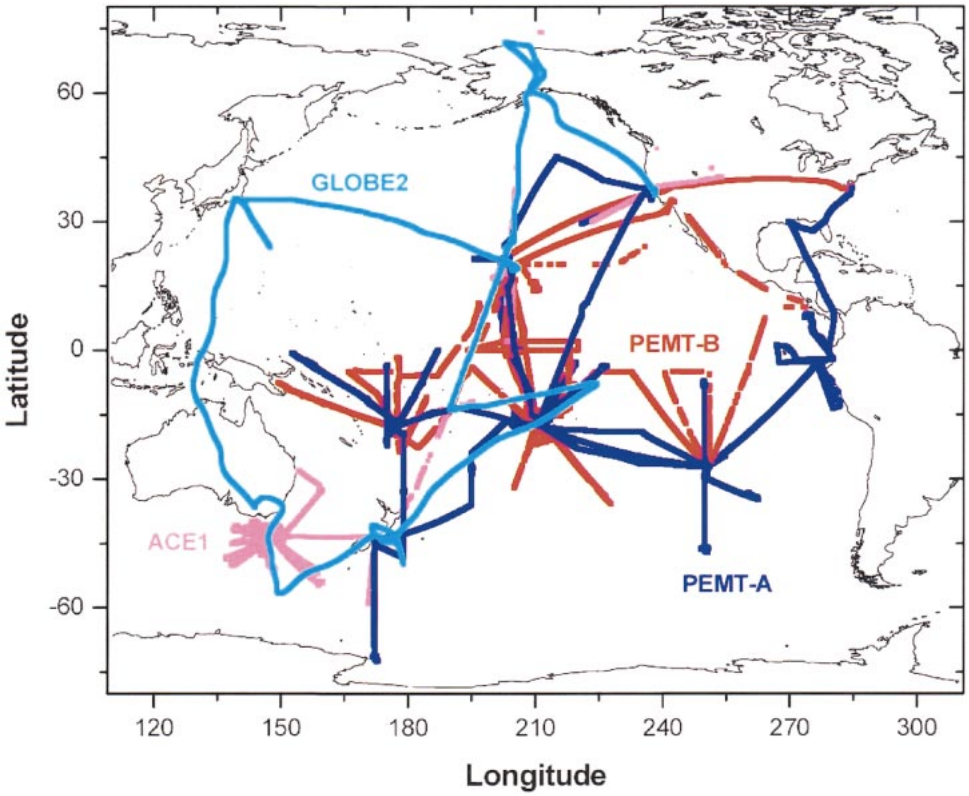

FIG. 1. Flight tracks over the Pacific for indicated aircraft missions and data used here. These include GLOBE-2 (May 1990, 15 flights, 37 profiles); ACE-1 (Nov 1995, 33 flights, 96 profiles); PEM-Tropics A (Sep 1996, 21 flights, 54 profiles); and PEM-Tropics B (Mar 1999, 19 flights, 35 profiles).

range of spatial and temporal scales, producing large aerosol datasets that provided empirical links between these properties and aerosol backscatter at various lidar wavelengths (Srivastava et al. 1997).

The Southern Hemisphere Marine Aerosol Characterization Experiment (ACE-1, 1995). Measurements made from the National Center for Atmospheric Research (NCAR) C-130 aircraft were designed to quantify the chemical, physical, and meteorological processes controlling the evolution and properties of the atmospheric aerosol relevant to radiative forcing and climate (Bates et al. 1998).

The Pacific Exploratory Missions [PEM-Tropics A (1996) and B (1999)] were gas and aerosol experiments that focused upon key factors controlling the chemistry of the atmosphere, its oxidizing capacity, and the nature of gas to particle conversion in the remote FT (Hoell et al. 1999; Fuelberg et al. 2000, manuscript submitted to *J. Geophys. Res.*).

b. Aircraft aerosol instrumentation

Aircraft measurements include aerosol size distributions, optical properties (light scattering and light absorption), and chemistry. The aerosol measurement systems were able to characterize aerosol concentrations and properties over all size ranges of primary interest to processes in atmospheric chemistry and aerosol physics (i.e., 0.003–20 μm). These included features ranging from aerosol nucleation, evolution of the size distribution, transport processes, and aerosol radiative effects. Thermal analysis (volatility) of size distributions allowed inference of aerosol physicochemistry and can distinguish aerosol with continental versus ''clean'' characteristics (Clarke 1991; Jennings et al. 1990). A summary of typical instrumentation follows.

1) A SIZE-RESOLVED THERMOOPTIC AEROSOL DISCRIMINATOR

In order to characterize the aerosol size distribution from 0.12 up to 7.0 μm—often where most aerosol mass, surface area, and optical effects are dominant—we have used a modified commercial laser optical particle counter (OPC) system to provide 256 size channels of data. A computer-controlled thermal conditioning system is used upstream of the OPC (airstream is dilution-dried) to characterize aerosol components volatile at temperatures associated with sulfuric acid and organics (150°C), ammonium sulfate–bisulfate (300°C), and refractory aerosol at 300°C (sea salt, dust and black carbon, flyash; Clarke 1991). Volatility observations can

be combined with bulk aerosol chemistry to generate size-resolved information of the composition, state of mixing, and refractive indices.

2) CONDENSATION NUCLEI—HEATED, UNHEATED, AND ULTRAFINE CONDENSATION NUCLEI

Two butanol-based CN counters (TSI 3010 and 3760) have been modified for aircraft use and count all particles between nominally 0.012 ± 2–3.0 μm. In this fashion we obtain total CN, refractory CN (RCN; those remaining at 300°C after sulfate is removed), and volatile CN (VCN; by difference) as a continuous readout. The ratio of RCN to total CN defines the RefRatio as an indicator of airmass variability since it is not directly dependent on aerosol concentration (Clarke 1993). We have observed that polluted and continental aerosol often have ratios near about 0.8 whereas more pristine regions tend to be far more volatile with low ratios often approaching zero (Clarke et al. 1997). Variability in the refractory component also appears to reflect sources of continental combustion (soot–black carbon, fly ash, some organics) or dust aerosol, whereas, in clean marine regions this component is generally lower (Clarke et al. 1997). The ''ultrafine CN'' (UCN) counter (TSI 3025) was used to count all particles between 0.003–3.0 μm. We also provide the differential measurement between CN and UCN instruments (UCN–CN) for particle sizes in the 3–12 ± 2 nm size range. Note that instrumentation evolved during our measurements over the past decade and CN counters (also sensitive to instrument temperature) effectively operated with lower detection limits that ranged from 0.01 to 0.15 μm depending upon instrument type and conditions. Rather than attempt to stratify the instrumentation and conditions we have elected to specify a nominal 50% size cut at 12 ± 2 nm for this paper. This and other minor instrumentation differences will not significantly alter the character or interpretation of the data presented here.

3) DIFFERENTIAL MOBILITY ANALYZER WITH THERMAL CONDITIONING

A modified differential mobility analyzer (DMA) with thermal analysis (see discussion for OPC above) provided size information (mass, surface area, number distributions) over the 0.01- to 0.25-μm size range (Clarke et al. 1998) for sampling times of about 1–3 min. This size range reveals much of the dynamic evolution of the aerosol in response to coagulation, growth, and cloud processing. Two DMA's in tandem were also often employed to select a size and then volatilize it to determine the size of any refractory component and determine the state of mixing of the aerosol.

4) NEPHELOMETER

A three-wavelength nephelometer (TSI 3560) with a 1-μm impactor cycled in and out of the inlet stream provided both total and submicrometer scattering values and coarse scattering (dust, sea salt) by difference.

5) ABSORPTION PHOTOMETER (PSAP–RADIANCE RESEARCH; DETECTION $< 1 \times 10^{-7}$ M^{-1} FOR 5-MIN AVG)

A continuous light absorption photometer was used to quantify the light absorption coefficient of the aerosol related generally to fine particle pollution black carbon concentrations but also associated with coarse particle dust. Data presented here reflects one or more sample leg averages of 20 min or more.

6) OTHER INSTRUMENTATION

PEM-Tropics B included both UCN sizing and sulfuric acid gas measurements. The UCN counter that provided resolution of the smallest detectable particles in the 3–4-nm size range was possible by custom pulse height analysis of a TSI 3025 UCN counter (Weber et al. 2000, manuscript submitted to *J. Geophys. Res.*, hereafter W2000). Sulfuric acid gas was also measured using mass spectroscopy (Eisele et al. 1993).

3. Aerosol survey data

a. GLOBE-2

The NASA GLOBE experiments (1989, 1990) aboard the DC-8 (Fig. 2) revealed large-scale features of the Pacific FT aerosol. Size distribution data from the OPC/Thermo. Optic Aerosol Discriminator instrumentation was used to calculate aerosol optical properties for direct intercomparison with the lidar backscatter signal (Srivastava et al. 1997; Cutten et al. 1996) while the CN and UCN counters were used to identify air mass characteristics that could reveal both regions of particle production and the relationship of aerosol properties to various meteorological conditions (Clarke 1993).

→

FIG. 2. The GLOBE flight from Darwin to Tokyo in the western Pacific exhibits the range of aerosol variability and scales. (a) False color lidar backscatter image for GLOBE-2 leg from Japan to Hawaii showing dust plumes over Japan spreading out over Pacific. (b) Ultrafine concentrations at about 8 km as a function of latitude showing lowest concentrations where aerosol mass and refractory aerosol mass are largest. (c) TCN and RCN as a function of latitude showing highest aerosol number volatility where UCN and CN are highest and lowest volatility in dust–pollution regions. (d) Similar detailed structure of aerosol fields vs latitude as exhibited in RCN to TCN ratio and UCN to CN ratio. These characteristics are more variable than concentrations alone suggest and show that aerosol types maintain their identity over relatively small scales even at 8 km.

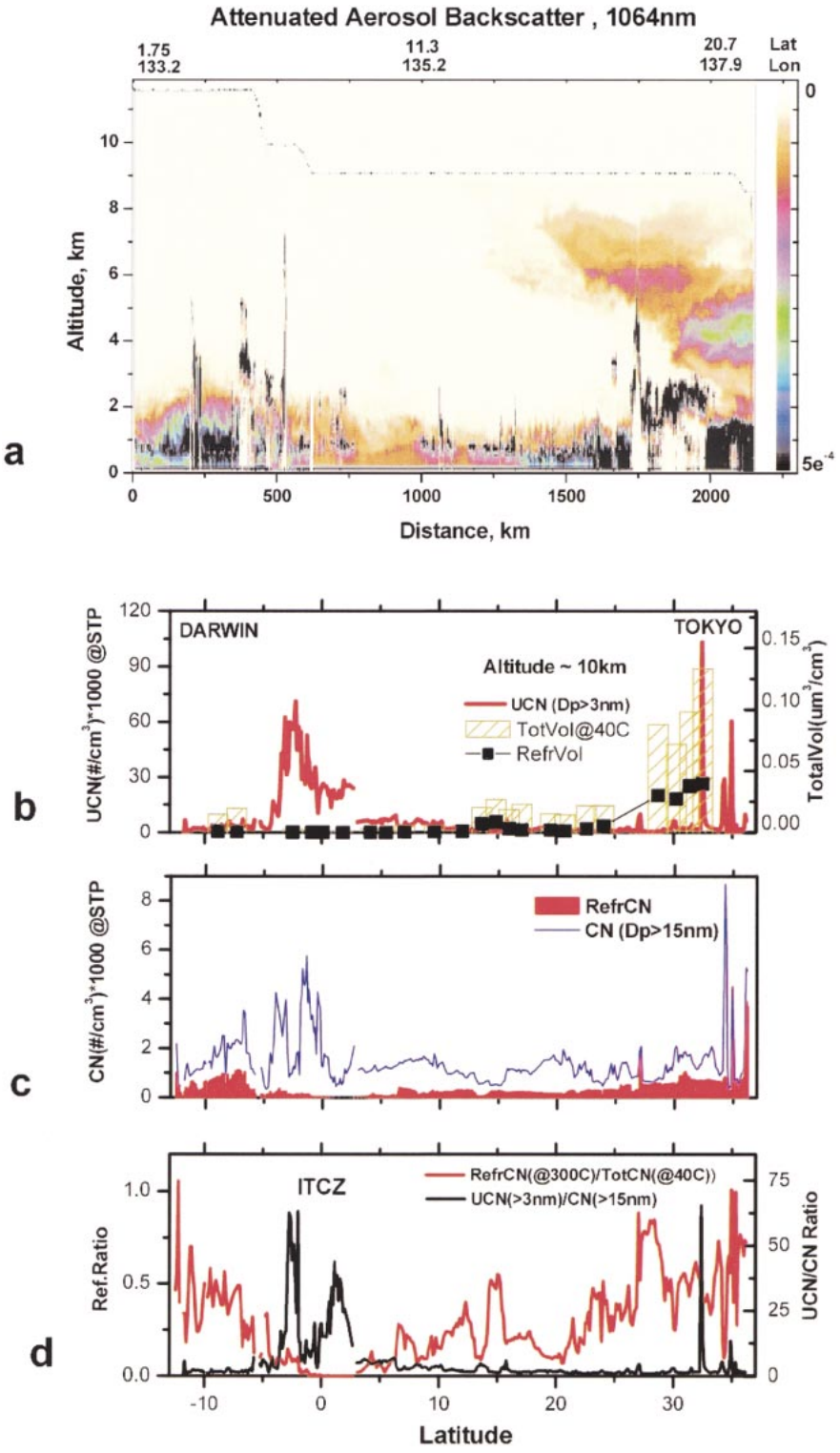
Attenuated Aerosol Backscatter , 1064nm
1.75
133.2
11.3
135.2
20.7
137.9
Lat
Lon
Altitude, km
Distance, km
a
DARWIN
TOKYO
Altitude ~ 10km
UCN (Dp>3nm)
TotVol@40C
RefrVol
UCN(#/cm3)*1000 @STP
TotalVol(um3/cm3)
b
RefrCN
CN (Dp>15nm)
CN(#/cm3)*1000 @STP
c
ITCZ
RefrCN(@300C)/TotCN(@40C))
UCN(>3nm)/CN(>15nm)
Ref.Ratio
UCN/CN Ratio
Latitude
d

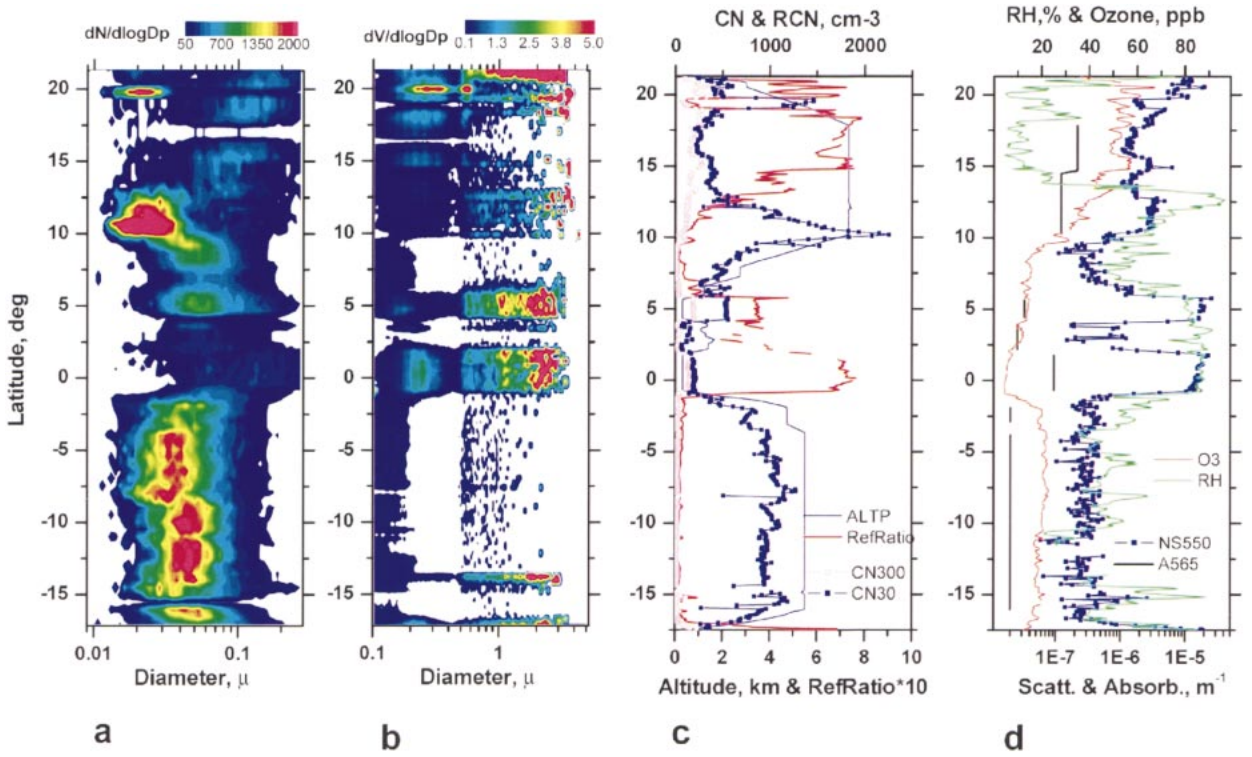

FIG. 3. Latitudinal structure of (a) RH, ozone, light scattering and light absorption, and (b) altitude, RefRatio, CN, and RCN. (c) Color-coded volume distributions obtained from OPC, and (d) color-coded number distributions obtained from DMA.

One example of the kind of data obtained is the GLOBE flight from Darwin to Tokyo in the western Pacific that exhibited the range of aerosol variability and scales suggestive of zonal features. The downward-looking lidar imagery for part of this flight between the equator and 23°N (Fig. 2a) reveals two intense dust plumes [one at 4 km (orange), another at 5 km (green)] near 20°N that extend further north over Japan for more than 1000 km of latitude (lower-level clouds are black). These originated over the Gobi Desert and are moving westward and out over the Pacific. On this flight (and others in the Northern Hemisphere) coarse dust particles aloft were generally found in very dry (<10% RH) air. In this case, variations in the size distribution (not shown) revealed the coarse dust aerosol mass present aloft changed to more submicrometer fine-mode pollution aerosol mass nearer the surface (<2 km altitude) during the vertical descent profile over Japan.

Particle characteristics of this northern dust plume can be contrasted with clean air encountered nearer the equator as seen in the three-panel time series for the same flight transect (Fig. 2b–d) from 15°S to 37°N. Most of the data was from near 8–9 km and the UCN, VCN, and RCN are indicated and identified in the caption. The fine structure in these measurements is real and provides a sense of the scales of variability to be found in the FT. Both VCN (volatile at 300°C) and UCN vary together while RCN (those remaining at 300°C) generally vary in an opposite sense reflecting their different origin. The greatest concentrations of ''new'' particles dominating the UCN are over the convective warm pool and approach 50 000 cm^{-3} near the intertropical convergence zone (ITCZ). These nuclei have since been shown to originate from gas to particle conversion in cloud outflow (see below). The highest concentration of new particles occurs in regions showing the lowest concentrations of surface-derived aerosol and that are also regions of lowest aerosol mass (Fig. 2b). The ratios of RCN to CN, and the ratio of UCN (>3 nm) to CN (>15 nm) (Fig. 2d) clearly show these trends as well as abrupt changes in aerosol character that are not evident in the concentrations themselves.

b. PEM-Tropics B

More recent experiments with additional instrumentation have characterized changes in the size distribution and other properties linked to both natural and continental emissions even in the remote equatorial central Pacific. Figure 3 is a flight from Tahiti to Hawaii with descents near the equator that provide a sense of the aerosol structure present in the remote troposphere. This flight also includes transitions between Northern Hemispheric and Southern Hemispheric air masses, as well as examples of various aerosol types that contribute to the data in this paper. The two leftmost panels show the color-coded number distributions from the DMA (Fig. 3a) that reveal the small particle features and the volume

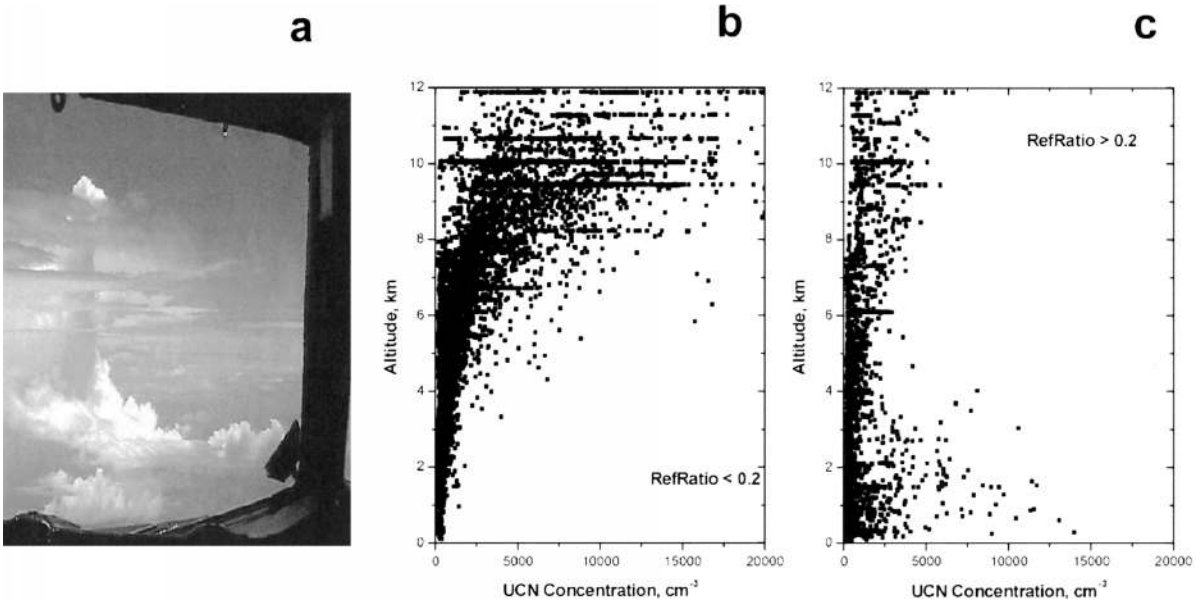

FIG. 4. New particles production: (a) example of multilayer vertical structure in the convective ITCZ, (b) vertical profiles of ultrafine CN concentrations for cases with RefRatio < 0.2, and (c) cases for RefRatio > 0.2 measured from P-3b and DC-8 during PEM-Tropics A–B.

distributions (Fig. 3b) from the OPC that reveal the larger particle features also as a function of latitude. Figure 3c shows a time series of altitude, CN, RCN, and RefRatio as functions of latitude, and Fig. 3d shows light scattering, light absorption (black carbon), ozone, and relative humidity. The ITCZ is located in the vicinty of 12°N at this time. Two low-altitude descents are made near 0°–5°N while the rest of the flight is near 6 km.

The low-altitude legs are typical of aged boundary layer with high RH coarse particle sea salt, high scattering but with some enhanced light aborption near the equator compared to 5°N that also shows up in the relatively high RCN; and aerosol volume near 0.2 μm. At high altitude in the Southern Hemisphere low and stable scattering, low and stable RCN, low RefRatio, low aerosol volume, and stable monomodal number distributions are evident with a gradual decrease in the mode diameter of the latter as we approach the equator. As will be discussed later, this 40–50-nm number mode is typical for clean subsiding air with volatile particles nucleated in the free troposphere.

Ascending to near the ITCZ near 10°S RH is seen to increase, CN increase to 2000 cm^{-3}, RCN drop to zero, and the DMA number mode moves to small sizes near 20 nm before RH approaches in-cloud conditions near 12°N. These increases in small volatile number are related to near-cloud nucleation discussed later. At the same time some coarse mode aerosol are seen to increase and ozone increases reflecting transitions to a different air mass. By 14°N, RH drops to 10%, CN drops, the DMA number mode increases to 100 nm, and these trends continue into the descent where coarse-particle dust and pollution (indicated by high absorption and high RefRatio) dominate the aerosol. However, even on the descent near 19°N we go through a 1-km-thick layer of clean air with enhanced small volatile CN before reaching the MBL.

These features will not be analyzed futher in this paper. They are shown here mainly to provide the reader with some understanding of the complex structure and variability present in the remote tropospheric aerosol and to provide an example of interhemispheric differences that are often evident. They also provide an example of the nature of the datasets that constitute the foundation of this paper.

c. Vertical distributions of aerosol number concentration

Experiments that followed the initial GLOBE observations focused on the processes that resulted in the natural production of the new particles in the FT. These confirmed that precipitating clouds removed aerosol mass and surface area to provide clean air aloft. Clouds also pumped reactive gases aloft into colder regions with high actinic flux that were more favorable for particle nucleation in cloud outflow (Clarke et al. 1998), as evident in concentrations aloft above the ITCZ (Fig. 2). These observations prompted other flights in the Tropics (PEM-Tropics A and B) where free troposphere particle concentrations were generally found to far exceed MBL concentrations (Clarke et al. 1999a).

Figure 4a shows the multilayer clouds characteristic of the ITCZ deep convection and multiple cloud outflow layers encountered during the most recent PEM-Tropics B experiment. This experiment focused upon gas and aerosol properties in the tropical regions. Figures 4b,c shows a superposition of all vertical profiles of UCN

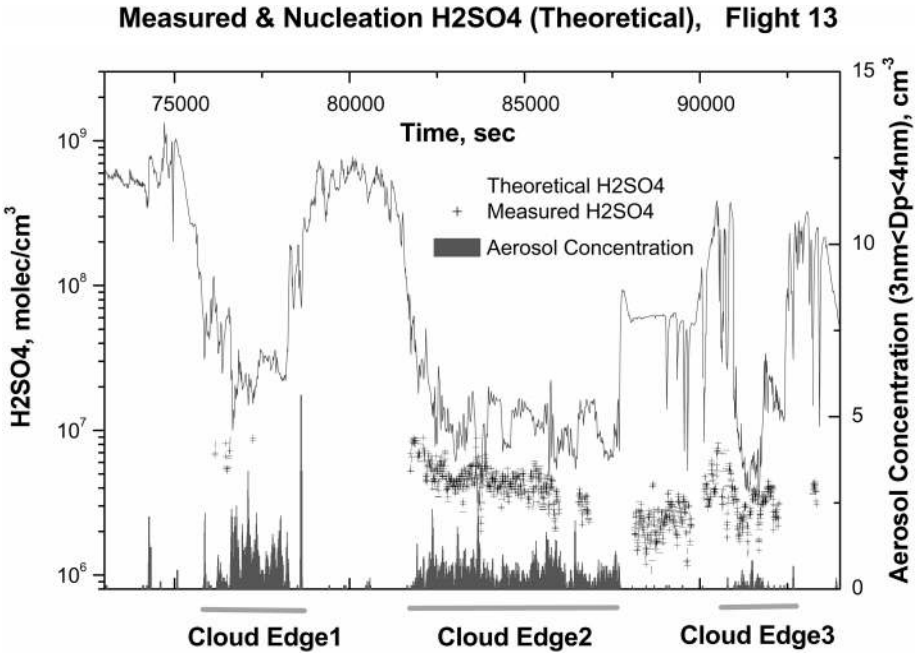

FIG. 5. Time series of three cloud-edge passes from PEM-Tropics B where recent nucleation can be seen in the 3–4-nm particle concentrations when measured sulfuric acid (+) approaches concentration needed for classical binary nucleation (line).

measured aboard the NASA P-3 and DC-8 aircraft in the Pacific Tropics. Here profiles have been plotted separately for UCN concentrations with RCN to CN (RefRatios) below 0.2 being indicative of clean conditions (Fig. 4b) and UCN concentrations for RefRatios above 0.2 indicative of continental influence (Fig. 4c). High RefRatios are characteristic of surface aerosol sources (dust, black carbon, sea salt). Clearly, particles with high RefRatios often dominate the tropical MBL below 2 km due to sea salt and at times the long-range transport of pollution during some PEM-Tropics flights near South America. Aloft the behavior is very different with most cases showing RefRatios less than 0.2 and exhibiting very high UCN. Lower UCN concentrations aloft that are associated with high RefRatios (Fig. 4c) include some cases with cloud pumping of poorly scavenged boundary layer air (sea salt) or more commonly cases of long-range transport of aged continental plumes (Moore et al. 2000, manuscript submitted to *J. Geophys. Res.;* hereafter M2000). These tropical data clearly demonstrate a high altitude source of new particles that can age and subside toward the boundary layer as well as a separate refractory near-surface source that can be mixed up into the upper layers.

An example from PEM-Tropics B for local conditions resulting in new particle formation is shown in Fig. 5 for P3-B flights near the edges of three ITCZ clouds (see Fig. 4a) when recent nucleation was observed. The solid line indicates the expected critical concentration of sulfuric acid needed for classical binary nucleation and that depends primarily upon ambient temperature and relative humidity (Wexler et al. 1994). When measured concentrations approach these values, then classical binary nucleation would predict nucleation. Recently formed nuclei in the 3–4-nm range (W2000) are seen to occur when the measured H_2SO_4 (Eisele 1993) approach these critical values within a factor of 2 or so. In order to be detected, particles will have nucleated earlier and grown to this minimum detectable size range over time so an exact agreement with critical sulfuric acid concentrations at the time of the particle measurements should not be expected. However, these new nuclei are primarily detected in regions of cloud outflow generally in the presence of sulfuric acid gas concentrations often consistent with binary nucleation (Clarke et al. 1999b).

d. Zonal structure of CN in the troposphere

These elevated concentrations of CN and UCN aloft were first observed on GLOBE (Clarke 1993) and more recently discussed in several papers referenced above have focused largely on the evidence for nucleation events on specific flights. Here we assemble all of our CN data from all five major aircraft experiments (Fig. 1) for various seasons during a 10-yr period in order to expose general features and large-scale aerosol processes active over the Pacific (Fig. 6). These many thousands of 5-min data points (see below) from altitudes above 3 km have been averaged here (Fig. 6a) over 2° latitude bands and plotted as refractory CN (RCN, $D_p > 12$ nm at 300°C), CN ($D_p > 12$ nm) and total nuclei

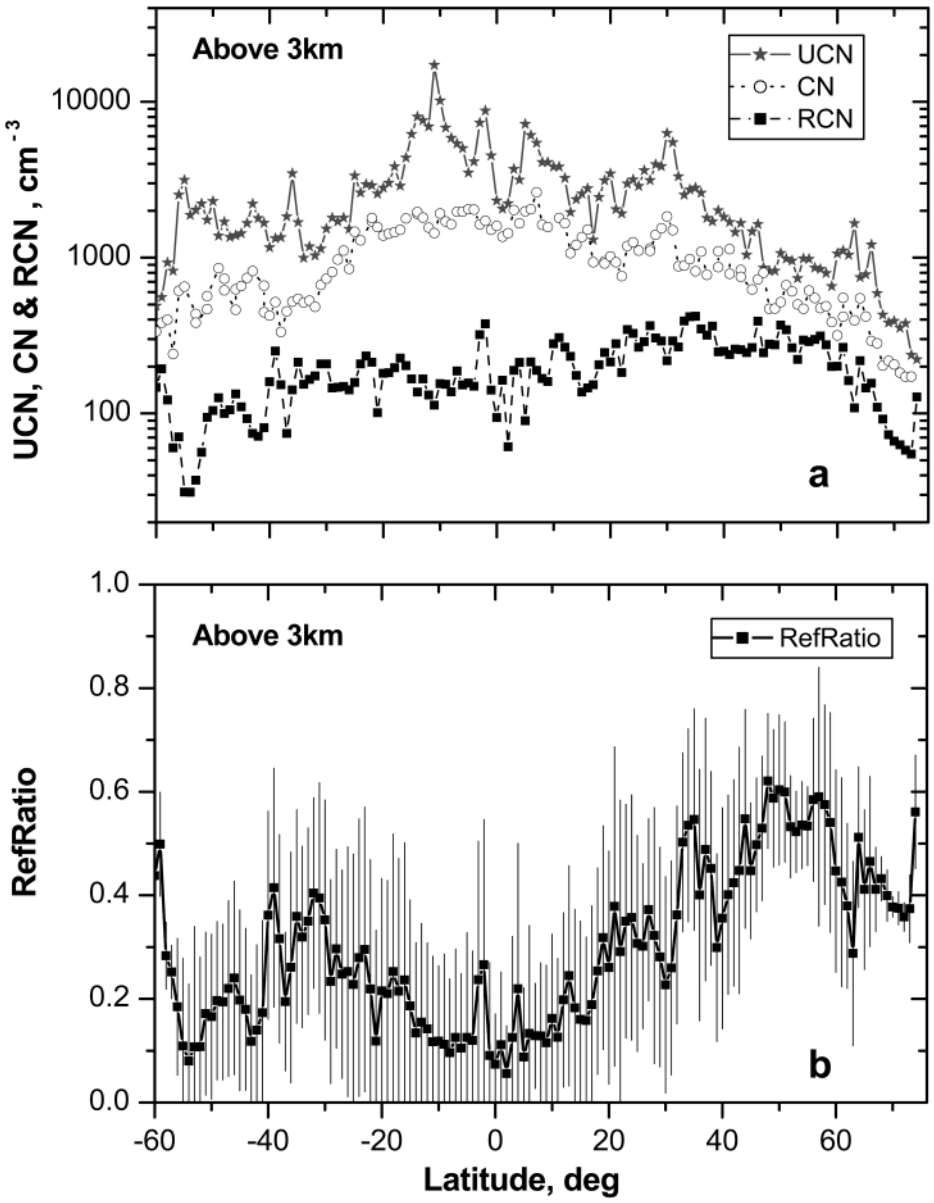

FIG. 6. (a) Latitudinal nuclei concentrations (UCN, CN, RCN) for all experiments (GLOBE-2, ACE-1, PEM-Tropics A and B) averaged over 1° latitude bands. Std dev have been left off for clarity but were typically about a factor of 3 for any given latitude. (b) Similarly for RefRatio, only with one std dev bar included.

measured by the ultrafine counter (UCN, $D_p > 3$ nm). Standard deviations (typically about a factor of 3) have been left off for clarity. Volatile CN can be estimated from the difference between the CN and RCN data. This clearly shows the enhancement in smaller and more volatile nuclei in the equatorial region where there is a deficit of surface-derived refractory aerosol. In Fig. 6b the relative contribution of these refractory CN to the total CN (RefRatio) have been also averaged along with one standard deviation indicated. The low RefRatio values near the equator also reveal the dominance of new volatile aerosol in this region. The RefRatio also demonstrates that surface-derived refractory nuclei are most common in the Northern Hemisphere and exceed typical values in the Southern Hemisphere by a factor of 2.

Figures 7a,b provide a latitudinal and longitudinal representation of the vertical distribution of total UCN aerosol concentrations in the vertical (5-min averages) and using a logarithmic color-coded concentration scale. The latter is dominated by data in the Tropics (Fig. 1) where high altitude data density is greatest. At other latitudes this data is limited due to lack of a high altitude

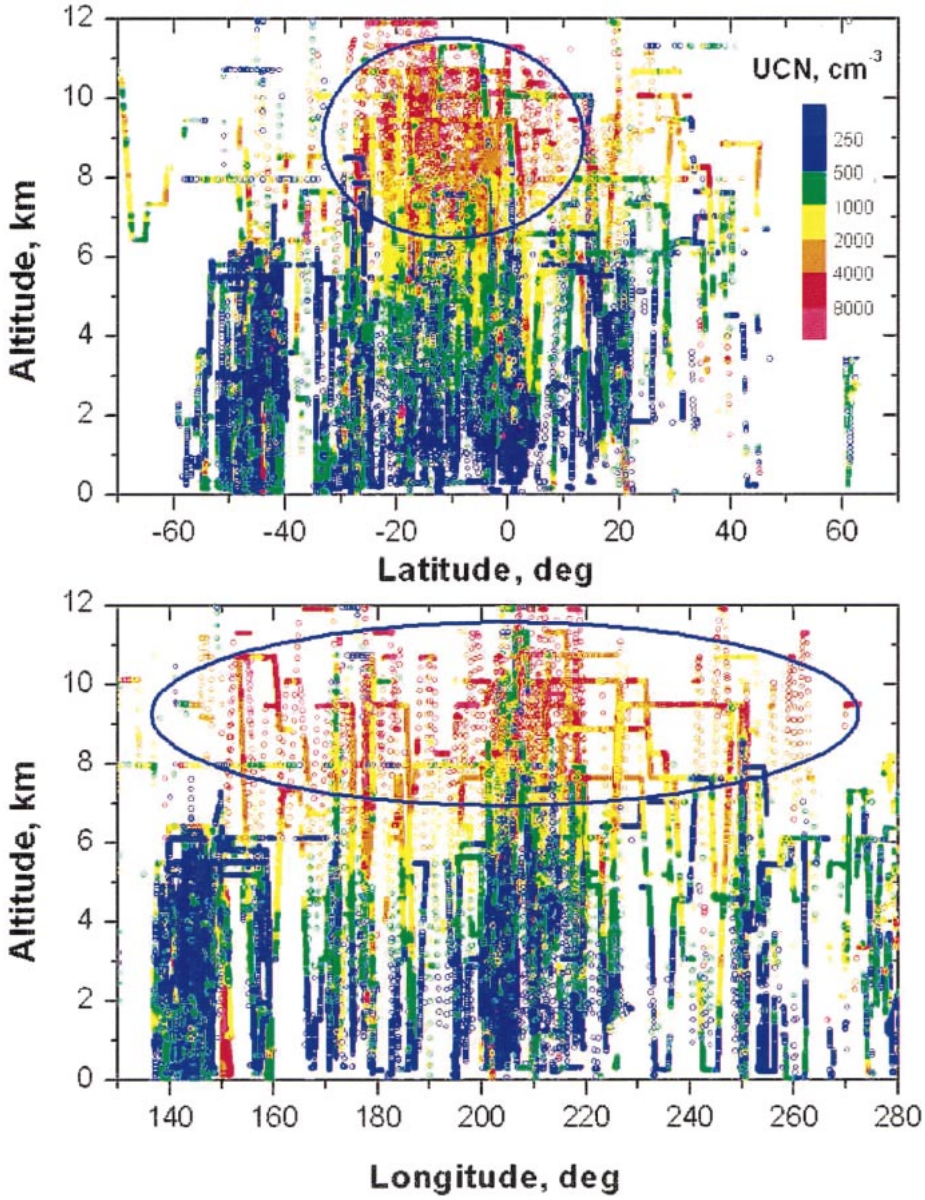

FIG. 7. Color-coded 5-min-average concentrations as a function of altitude and (a) latitude and (b) longitude for all experiments. Highest concentrations are found aloft and distributed over the equatorial zone of deep convection.

aircraft, but the elevated UCN concentrations are still most common. The longitudinal presentation (Fig. 7b) shows that the high concentrations linked to tropical convective outflow (Fig. 5) persist over the entire tropical Pacific. Both figures show concentrations decreasing toward the surface.

For clarity, the data shown in Fig. 7 are broken into three panels (Figs. 8a–c) that cover three concentration ranges (0–500, 500–2000, 2000–10 000 cm^{-3}). The first range is typical of CN present over the remote oceans in the MBL while the upper range is most commonly observed near regions of recent nucleation in the vicinity of deep convection (or in regions of pollution when the RefRatio is high). The intermediate range can represent both aged CN from new particle production (low RefRatios) and concentrations often present in aged pollution plumes (RefRatio approaching 1). Between 20°N and about 20°S the upper troposphere exhibits the highest concentrations of UCN. These appear to be linked to deep convection over both the ITCZ and the South Pacific convergence zone that enhance production aloft. This points to the significance of deep convection in the global particle budget by providing a means for removing high aerosol mass and surface area but replen-

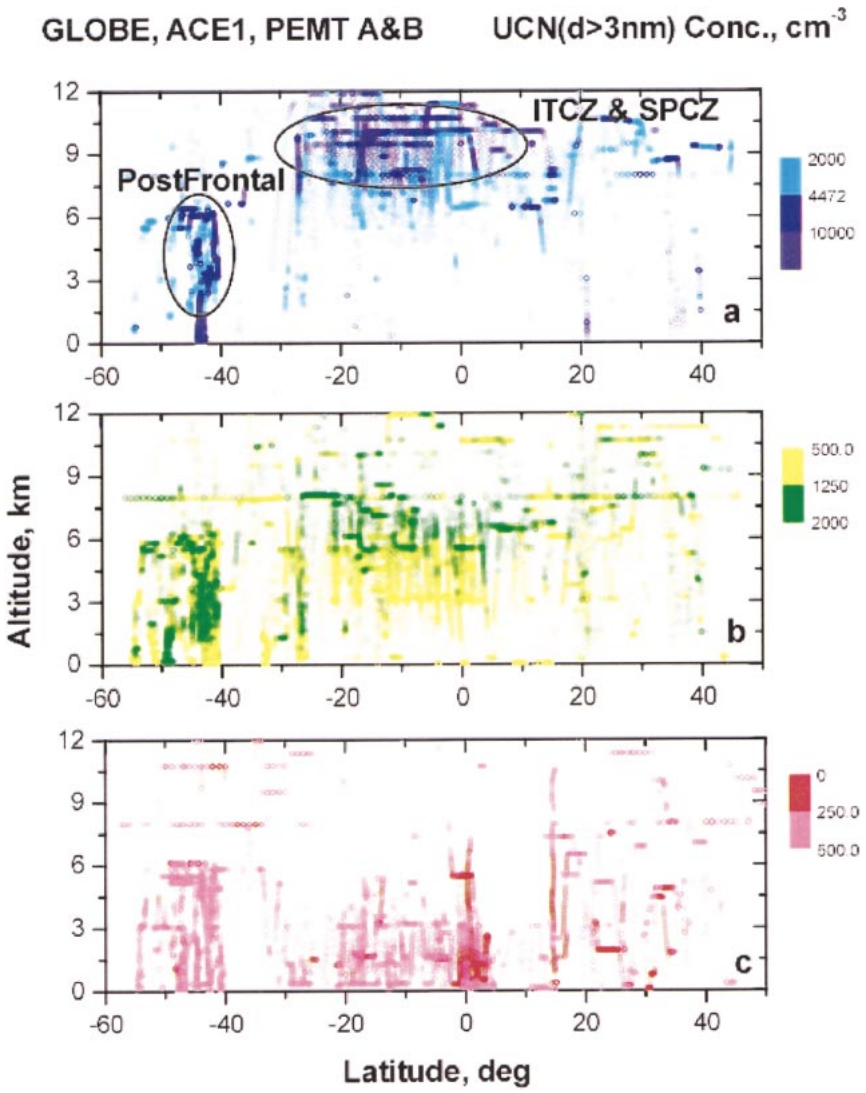

FIG. 8. For clarity the regions shown in Fig. 6 as function of latitude are broken out into locations where low (0–500), medium (500–2000), and high (2000–10 000) CN concentrations were measured. Note high concentrations near 45°S from ACE occur at about half the altitude of similar tropical concentrations and tend to mix to the surface in postfrontal activity.

ishing the scavenged air mass with high concentrations of new and smaller nuclei. At higher latitudes in both hemispheres, lower concentrations are more evident.

Figure 9 provides a sense of latitudinal differences in vertical profiles of UCN averaged over 1-km altitudes for the latitude bands 20°S–20°N, 20°–70°N, and 20°–70°S. All profiles show order of magnitude increases of concentrations with height. Although variability at any altitude is clearly significant, UCN aloft are clearly enhanced in the 20°S–20°N region relative to higher latitudes. Below about 6 km, the equatorial and Northern Hemisphere regions are similar, but the southerly region is enhanced in UCN by about a factor of 2. However, these data are dominated by the ACE-1 data south of Tasmania and may not be representative of the southern latitude band as a whole. In spite of fewer high altitude flights in higher latitude regions it appears likely that these differences reflect air masses less influenced by nucleation in clean air and also decoupled from the tropical latitudes, as might be expected for typical characteristics of the Hadley circulation.

The high concentrations associated with convective regions near the south polar front (ACE-1) are also well scavenged air masses with very low particle surface area and new particle production that appears to be linked to cloud pumping of precursors aloft where low surface area, low temperatures, and high humidity favor sulfuric acid nucleation, as shown in Clarke et al. (1998). This convection is in colder regions that are characterized by frontal activity and vertical motions that generally do

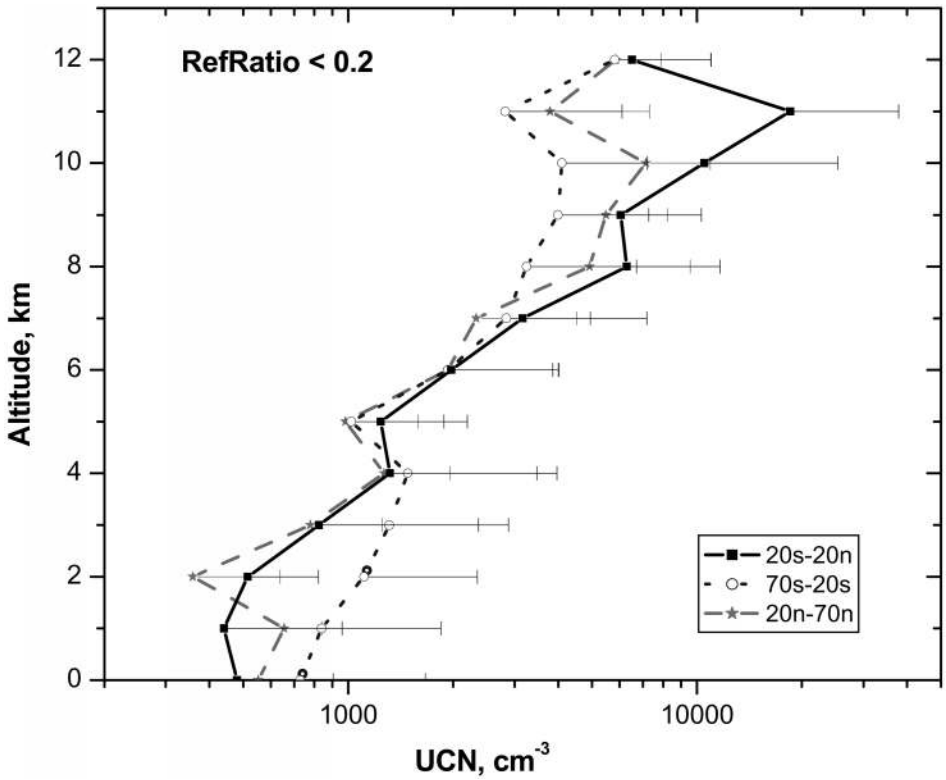

FIG. 9. Vertical profiles of UCN data (at STP) from Fig. 6 averaged for latitude bands 70°–20°S, 20°S–20°N, and 20°–70°N. Positive std dev only are indicated for clarity. Average aerosol concentrations increase with altitude at all latitudes by about an order of magnitude, by about 10 km, but equatorial concentrations aloft are the highest.

not rise as high as in the Tropics (see Fig. 8). Unlike the ITCZ clouds, during the ACE-1 period, the deep convection of up to 6 km tended to be more isolated clouds embedded in larger cloud fields with tops below 4 km. However, as discussed in conjunction with Fig. 5, binary nucleation of sulfuric acid is commonly found to depend upon temperature and RH (Wexler et al. 1994; Clarke et al. 1999b). Assuming sulfuric acid is not limiting and since cloud edges always approach 100% RH, it appears that when photochemistry is similarly active, then temperature is the remaining key environmental parameter that can promote nucleation. If we reexamine the profiles for this ACE-1 data and the PEM-Tropics A and B tropical data (Fig. 5) replotted as a function of temperature (Fig. 10) instead of altitude, all profiles reveal similar features as a function of environmental temperature. Under favorable conditions, active nucleation appears to increase in all profiles as temperatures drop from about 280 to 220 K, suggesting that temperature may be a useful parameter to model the conditions controlling nucleation from cloud outflow in diverse regions. The high concentrations at low altitude (T near 280°C) identified as ''mixing'' in the ACE-1 profiles originate from only two flights when we flew in postfrontal subsiding air that brought these new aerosol down to the surface (Bates et al. 1998). Because lower temperatures and nucleation events are found much closer to the inversion in the higher latitudes, it can be expected that such events will play a more active role in mixing the newly formed particles near 3–6 km back down toward the surface (Covert et al. 1996; Clarke et al. 1998; Bates et al. 1998; Brechtel et al. 1998; W2000), compared to the tropical environment.

e. Vertical structure of aerosol size distributions and entrainment into the MBL

The observations above provide insight into the regions of natural aerosol production in the Pacific troposphere, but they do not characterize the evolution of these aerosol. In order to explore processes linked to the formation, growth, evolution, and removal of tropospheric aerosol, one can examine associated variations in the aerosol size distributions. In view of the large extent of the tropical Pacific, and because PEM-Tropics focused on central Pacific tropical region with extended aircraft measurements in the free troposphere, we will describe this aerosol in some detail.

A picture of the vertical distribution of particle number distributions in this equatorial zone is provided by a composite of six profiles of DMA data (Fig. 11a) obtained during PEM-Tropics B between 20°N and 20°S

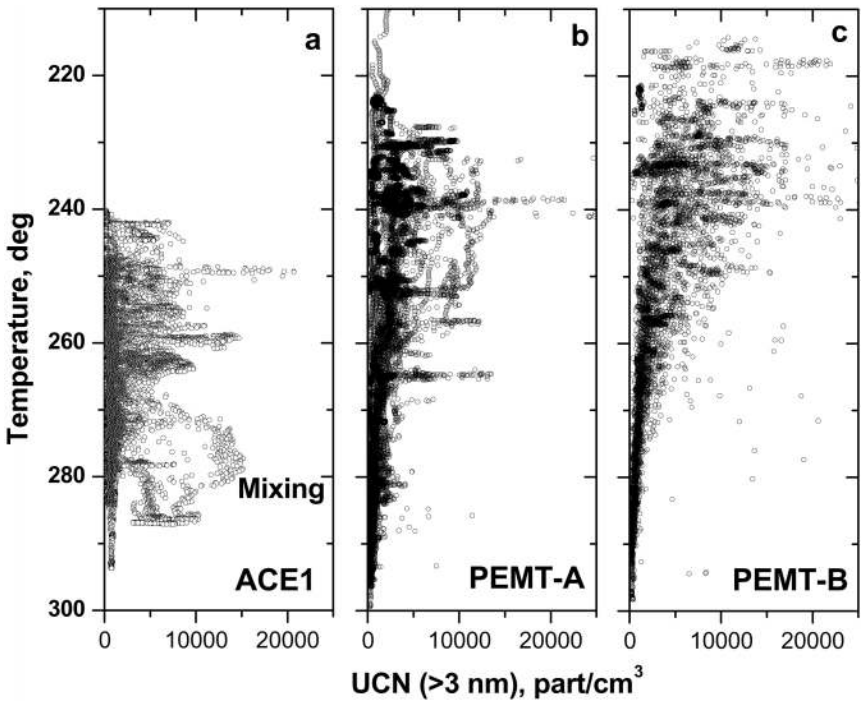

FIG. 10. Vertical profiles of UCN for equatorial profiles on PEM-Tropics A and B, and midlatitude date from ACE-1 field missions plotted as a function of ambient temperature instead of altitude. This reveals similarities in temperature dependence on the nucleation process in spite of large differences in actual altitudes evident in Fig. 5.

during March 1999 (P-3b flight numbers 5, 6, 8, 9, and 15). These were from different days and locations, and not all altitudes were equally sampled, but a similar number of distributions have been used here to describe each altitude range. A 2D smoothed representation of this data is included for clarity in Fig. 11b. Highest number concentrations of smallest particles are present at 7.5 and 8.5 km (only two profiles went above 6 km) and reveal recently formed smaller nuclei with diameters near 0.02 μm superimposed on the more aged distribution with sizes in the range of 0.05 μm. During the descent below 5 km, aerosol concentrations (at STP) decrease but gradually shift to larger sizes probably due to a combination of coagulation, mixing, and growth. Below about 2 km the aerosol can encounter low-level clouds in the so-called buffer layer (around 800–1800 m) and even more frequently in the surface mixed layer (around 0–800 m). The monomodal distribution in the FT becomes somewhat larger and shifts to a bimodal distribution in the surface mixed layer with a minimum present near 0.08–0.09 μm. This is consistent with the intermode minimum associated with cloud processing of aerosol through nonprecipitating clouds (Hoppel et al. 1986, 1990) common to this tropical region. This minimum is the same size as we have observed during equatorial measurements at Christmas Island and which led to the suggestion of a possible monomodal aerosol aloft being entrained into the MBL (Clarke et al. 1996).

The location of the minimum suggests average MBL cloud supersaturations of about 0.4 for this regions and vertical velocities near 1 m s^{-1}. In the MBL this process preferentially increases the mass of the larger aerosol activated to cloud droplets due to greatly increased surface areas and rapid aqueous reaction rates. Note that the smallest sizes of particles in the MBL are slightly larger than those immediately above the MBL, indicating that these are entrained from above rather than being nucleated and growing independently in the MBL. This averaged tropical profile suggests formation of new particles aloft followed by slow growth during subsidence, entrainment, cloud processing, and more rapid growth in the MBL (Clarke et al. 1996; Raes 1995). This process is also coupled to the cycle that results in the aged and higher concentrations of accumulation-mode aerosol evident in the equatorial region (Quinn et al. 1996).

f. Vertical profiles of integral properties in the Tropics

Number size distributions such as those shown in Fig. 11a can be integrated to obtain total number, surface area, and volume (or mass). This has been done for the combined DMA and OPC size data ($0.01 < D_p < 5$ μm) for the measured ''dry'' aerosol for all PEM-Tropics (autumn) and PEM-Tropics B (spring) data. Data has been stratified onto clean naturally sourced aerosol versus continentally influenced based upon RefRatios less than or greater than 0.2, respectively. Justification for

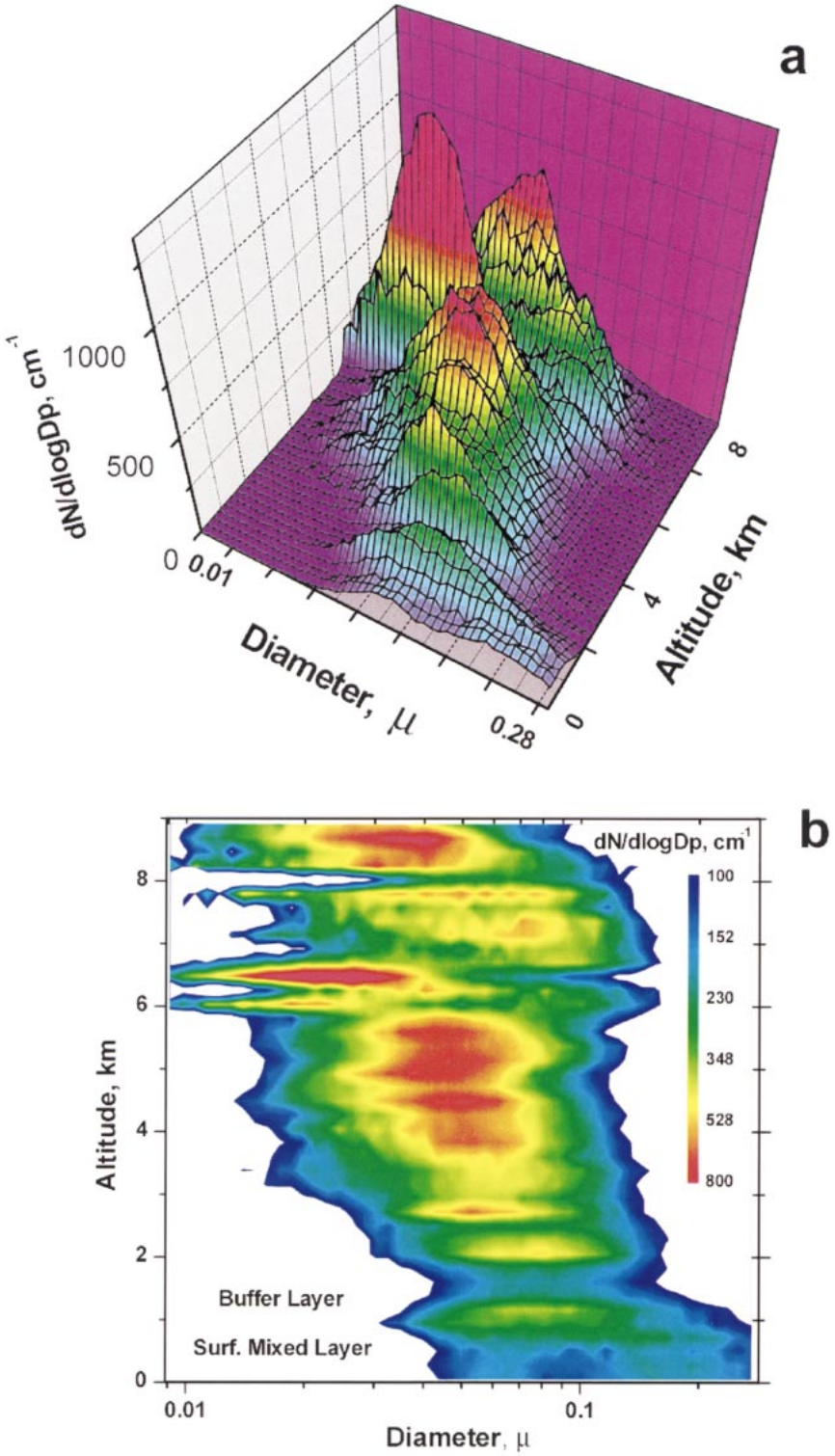

FIG. 11. Vertical profiles of DMA number size distributions from six PEM-Tropics B equatorial profiles between 20°S and 20°N showing high concentration of CN and recently formed small nuclei aloft that appear larger at lower altitudes and develop bimodal features in the cloud processed MBL.

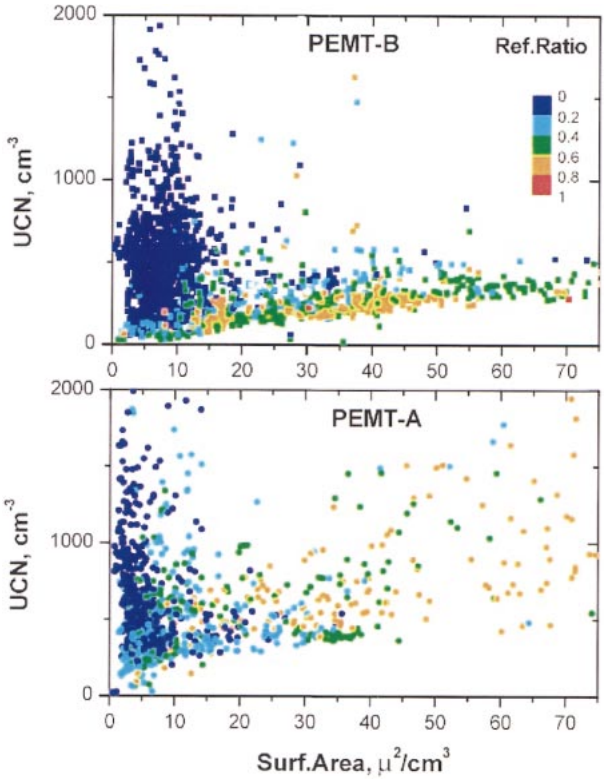

FIG. 12. Plot of UCN vs DMA–OPC surface area, color-coded by RefRatio. Two aerosol regimes are indicated (clean vs continental). The RefRatio value of 0.2 appears to serve well to identify them and forms the basis for using this value in this paper.

this is evident in the plots of UCN versus surface area for both PEM-Tropics A and PEM-Tropics B shown in Fig. 12. Generally RefRatios less than 0.2 dominate cloud-scavenged air with low surface area. Values greater than 0.6 suggest a clear continental dominance, while values between 0.2 and 0.6 can be mixtures of the clean and continental cases or near-surface regions with greater sea salt contributions. The greater scatter and higher UCN for higher surface areas in PEM-Tropics A compared to PEM-Tropics B reflect the greater frequency of higher altitude aged plumes and mixed aerosol on PEM-Tropics A. In most cases this refractory component increases with black carbon (in soot) (M2000) and dust (although total number concentrations in dust-only events are generally low). Hence, the high RCN here generally reflects a surface-derived combustion aerosol.

This stratification of the data using the RefRatio threshold of 0.2 has also been applied to the light scattering data for the PEM-Tropics missions to identify clean and continentally influenced air. Figure 13 shows panels of scattering values for PEM-Tropics A and B for both cases. The lower panel shows the mean values and standard deviations as a function of altitude for both experiments and both stratifications. About an order of magnitude difference in scattering is evident between the so-called clean and continentally influenced air masses. These 5-min averages include more data points than the DMA–OPC size data, but the overall vertical structure in clean and continental cases is similar to aerosol volume profiles than surface area (see below). Below

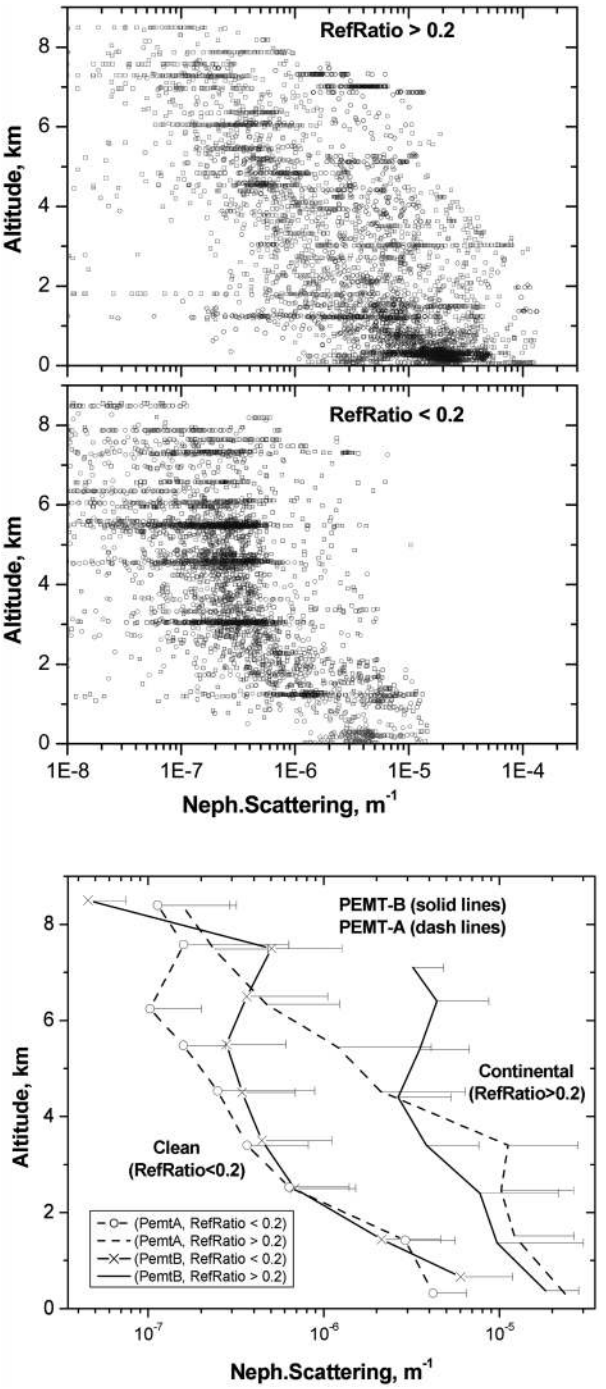

FIG. 13. (a) Plot of all light-scattering data from PEM-Tropics A and B for values of RefRatio above 0.2 (clean) and below 0.2 (continental influence). (b) Averaged vertical profiles of same for both PEM-Tropics A and B showing positive std dev only for clarity. About one order of magnitude separates clean and continental cases.

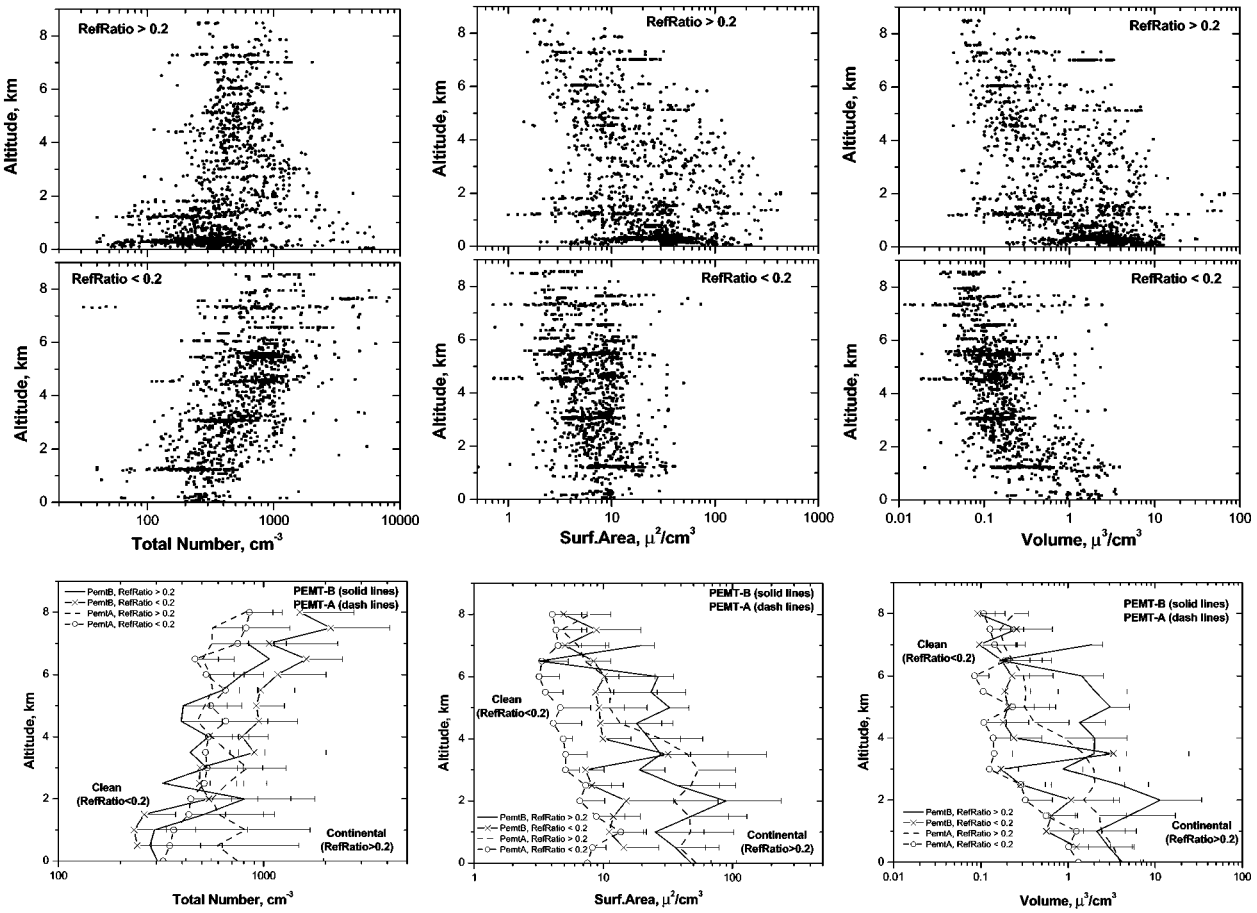

FIG. 14. Vertical profiles number, surface area, and volume integrated from aerosol size distribution data and coded with RefRatio to reveal typical range clean and ''perturbed'' aerosol measured over the Pacific on PEM-Tropics A and B. High RefRatio generally indicates continental pollution plumes (soot and dust).

4-km PEM-Tropics A and B scattering are similar for both the clean and the continental profiles. However, above that altitude PEM-Tropics B values are larger and appear dominated by two flight legs of higher aerosol volumes evident in the scatterplots in Fig. 14.

In Fig. 14, integral values of total number, area, and volume are shown for all of PEM-Tropics A and B for both ranges of RefRatio in the upper (continental) and middle (clean) panels, while the lower panel reveals the average values and standard deviations of the data for each of these cases. Only one leg of the standard deviation is shown for clarity. All concentrations for number, surface, and volume have been corrected to STP so that changes in concentrations with altitude reflect real changes in effective ''mixing ratios'' allowing different altitudes to be compared without regard to pressure considerations. Data from extended horizontal flight legs, but with variable concentrations, are often evident as an organized linear range of data points at a fixed altitude present in all plots. Data shown are for dry aerosol sizes measured at about 40% instrument RH in the MBL or lower aloft. Due to water uptake at higher ambient humidity typical of the MBL (say 75%), estimates of ''ambient'' MBL sizes, surface areas, and volumes should reflect increases in diameter of about 1.3, surface area of about 1.7, and volume of about 2.2 compared to values present in Figs. 9a–c. However, at higher altitudes where RH values are often lower the increases to ambient sizes will be generally much less.

Starting with the number distributions in Fig. 14 we see that total number concentrations increase significantly with height for both PEM-Tropics A and B, for the clean cases with low RefRatios. Above the MBL, the continental cases show less increase with height and concentrations aloft are generally lower than clean concentrations at the same altitude. This suggests that the presence of continental aerosol tends to result in reduced concentrations of aerosol number aloft. The relatively fewer cases of low RefRatio data (clean) below 2 km is due in part to the ubiquitous presence of refractory sea salt near the surface that when mixed with the subsiding aerosol raises the combined RefRatio from our clean to continental category. The overall lower number concentrations near the surface also reflect the more

active aerosol removal processes in the MBL. Hence, we will focus here on the FT data above 2 km.

Surface area plots suggest that values in the cleanest air above the MBL lie in the 2–20 μm^2 cm^{-3} range for clean cases and show little variation with height. The continentally influenced values tend to be in the 10–100 μ^2 cm^{-3} range, just above 2 km, and drop to near-clean values at 8 km. The average difference between clean and continental aerosol surface area measured over this altitude range is about a factor of 4 with greater differences in the PEM-Tropics A cases (more continental influence) compared to PEM-Tropics B.

The volume plots show that average volume in the clean case tends to decrease with height up to about 3–4 km, consistent with the trend to smaller sizes evident in Fig. 11, in spite of increasing numbers with height. This suggests that while coagulation may reduce the number of these clean nuclei during subsidence heterogeneous gas-to-particle conversion must be also adding mass to these particle during the process below about 4 km. It is also possible that cloud outflow at lower altitudes may typically yield fewer initial nuclei than would nucleate at the colder temperatures present at higher altitudes. At the same time lower altitude clouds may actually detrain more gas phase precursor such that resulting particle sizes and total mass are greater. It is possible that both process may be at work. The few unusually high values for surface and volume near 2 km are for an Asian dust–pollution outbreak in the Northern Hemisphere encountered near Hawaii on the return PEM-Tropics B flight (C01).

g. Long-range transport

In the discussion above we have focused upon larger-scale features of aerosol in the troposphere that reveal the interplay between both natural in situ aerosol sources and surface-derived sources. Continental surface sources, including anthropogenic, have been shown to contribute both to MBL and FT aerosol and express themselves with a high RefRatio and elevated scattering and absorption due to the presence of combustion products that include black carbon (Clarke 1989). There are many examples of continental aerosol detected over remote regions (Duce et al. 1991; Anderson 2000; Jaffe et al. 1999). However, there are few cases that illustrate the transport mechanisms associated with these events on global scales and over thousands of kilometers. The introductory data from GLOBE (Fig. 2) and PEM-Tropics B (Fig. 3) reveal a few aspects of this long-range transport for dust and pollution and links to the measurements we have discussed here. Our reference here to continental sources did not distinguish between issues such as the transport of dust and or pollution or the character of the size distributions for these species, including mass estimates of volatile and refractory components. Hence, our treatment here reduced these properties to integral characteristics that could be used to compare to the so-called clean natural sources in the troposphere. However, the experiments discussed here do have a substantial body of data on aerosol properties directly related to long-range transport in both the FT and MBL. One example includes the FT transport of Asian dust and pollution to the central Pacific and its entrainment into the MBL (C01). Another provides aerosol data demonstrating long-range transport over 5000 km in the MBL that is consistent with similar inferences from gas phase measurements (Jacob 2001). We are presently developing an assessment of such events (M2000) and related aerosol properties including inferred concentrations of black carbon, sulfate, the ammonium/sulfate molar ratio, volatile and refractory aerosol mass, scattering and absorption coefficients, potential CCN, etc. and their links to sources and gas phase species. The evaluation of these data and their statistical significance will be the subject of a paper that will be Part II in this Pacific aerosol survey.

4. Discussion

The assembly and evaluation of hundreds of flight-hours of aerosol measurements over the Pacific have provided insight into the processes linked to the transport and evolution of aerosol. A globally significant aerosol source in the FT is associated with particle nucleation from cloud outflow and characterized by its volatility. Aerosol formed near these convective elements are eventually returned to the surface generally via compensating large-scale subsidence during which the concentrations decrease through coagulation. The relatively narrow convective equatorial region is a major source region for these aerosol, and these data suggest the impact of this process on nuclei in the FT is expressed over latitude scales similar to the Hadley circulation.

The relative contribution of these natural aerosol as opposed to continental aerosol to FT concentrations was gauged by the ratio of RCN to TCN present. When plotted versus latitude this average ratio indicates a tropical zone dominated by volatile natural CN ($>$80%), a Northern Hemisphere showing about a 50:50 mix of natural and continental, and a Southern Hemisphere natural fraction of about 70% with somewhat higher fractions over the Southern Ocean. However, large variability could be expected at any location. Largest variability in the ratios were evident in the vicinity of 25°N and 20°S and probably reflecting active transition regions separating equatorial and midlatitude air masses.

This upper FT nuclei source was demonstrated to result in a gradient in number concentration from aloft toward the surface. Upon approaching the MBL inversion near 2 km these natural and volatile aerosol with low RefRatio markedly increase their surface area and volume. After mixing into the MBL those particles with sizes above about 0.8 μm are activated in MBL clouds and continue to add mass heterogeneously more rapidly

than unactivated sizes to result in a minima near this size. The small size of these aerosol naturally formed aloft increases only slowly during descent to the MBL, where more rapid growth is evident. About one order of magnitude volume added to these aerosol below about 2 km (see Fig. 14) suggests that near-surface sources in remote oceanic regions [e.g., dimethylsulfide (DMS) oxidation] probably convert the majority of available mass to aerosol heterogeneously in the MBL with significantly less exported aloft by convection. In spite of the large number of particles formed aloft, because of their size, very little precursor material is needed for their genesis. The little change in average integral mass evident for these subsiding clean aerosol above about 4 km suggests that the source strength of precursor gases is generally weaker above 4 km compared to below. This may imply that convection and cloud detrainment below this altitude may be more significant for the mass flux of gaseous precursors (e.g., DMS) pumped out of the boundary layer by clouds even though production of aerosol number is clearly greater farther aloft.

These naturally formed and subsiding aerosol in the Tropics can play a significant role in the cycling of CCN in this region. For the average particle size profile shown for the Tropics (Fig. 11) about 1/3 of the number of particles near 2 km are larger than 0.08 μm and therefore immediately effective as CCN for the supersaturations evident (about 0.4) for the MBL clouds in this region. This profile is very similar to the single ACE-1 profile in this region from 1995 (Clarke et al. 1998). The intermode minimum is also the same as observed at Christmas Island during our ground-based entrainment study in 1994 (Clarke et al. 1996) and the monomodal distributions above the inversion with bimodal below are virtually identical to those also measured in the extensive subsidence region near Hawaii (Clarke et al. 1996). This close similarity in these key features indicates that this process is representative of similar and persistent entrainment over extensive regions in the Tropics and subtropics. Hence, the entrainment estimates obtained from the Christmas Island experiment are expected to be representative of these extended regions. A typical entrainment velocity for an inversion height near 1500 m was determined to be about 0.6 ± 0.1 cm s^{-1} and suggested a replenishment time for MBL aerosol of about 3 ± 1 days (Clarke et al. 1996).

Given the FT size distributions and concentrations measured just above the inversion on PEM-Tropics B (e.g., Fig. 11) this provides an estimate of the flux of CN and CCN into the MBL in the Tropics and subtropics. A typical concentration above the inversion near 2 km for the clean unperturbed case is about 450 cm^{-3} (Fig. 14). As mentioned above, about one-third of these, or 150 cm^{-3}, would be immediately available as CCN in the MBL, once entrained. Hence, assuming particles are well-mixed after entrainment, about 150 CN cm^{-3} and 50 CCN cm^{-3} day^{-1} should typically be added to the MBL. The actual number of CCN is probably higher since cloud processing will slowly add mass to the swollen but unactivated interstitial aerosol while they are in cloud and gradually move them into sizes where they will become activated in following cloud cycles. Of course, some will be lost through coagulation, collision–coalescence, and removal via precipitation. Hence, this natural source of particles nucleated in cloud outflow aloft evolves to provide a significant natural source of MBL CCN independent of sea salt and continental sources.

Although synoptic and environmental conditions driving convection in the Tropics and in higher latitudes are different, the processes linked to aerosol formation appear similar. When profiles of elevated nuclei were compared for the Tropics and the ACE-1 study in the Southern Hemisphere the altitudes for apparent nucleation were higher in the Tropics. However, when expressed as a function of temperature instead of altitude then evidence of production through nucleation were very similar. This suggests modeling new production parameterized by temperature may be a suitable approach when precursor species are being lofted by convection. Subsidence and mixing into the MBL was also evident in the ACE-1 data but appeared more episodic and associated with postfrontal subsidence enhanced by the production of new particles aloft that were closer to the top of the MBL. Lifetimes and evolution in this higher latitude MBL can be expected to be quite different compared to the Tropics due to the rapid (about 3 days) sequence of frontal passages and more active precipitation common to this regions.

Relatively low CN number concentrations (about 500 cm^{-3}) are seen to be generally near the surface except in the North Pacific FT, where continental aerosol, often with low number and high mass, is often present. These features are occasionally evident at other latitudes and are associated with other plume advection from the continents (M2000). These continental aerosol are often internally mixed with a refractory (nonvolatile) residual indicative of combustion (black carbon, fly ash, and some organics) with volatile surface components (sulfate, etc.). In the North Pacific spring, these combustion-derived aerosols are also often found associated with the same meteorology that transports ''dust events.'' The FT in the subtropics often shows frequent and marked transitions and mixing between these clean and continental aerosol types.

Other aerosol types sourced at the surface such as continental and/or pollution aerosol generally exhibit higher values of the RefRatio. Refractory components in the MBL with values near 0.5 can also reflect a mix of sea salt and naturally sourced aerosol. These three sources (natural, sea salt, and continental) determine the properties of the MBL aerosol RefRatio found at all locations. When surface-derived aerosol is evident it was shown to generally dominate aerosol surface area, volume, and light scattering but usually not number. Plots of number against surface area demonstrated that

new particle formation aloft is highest for surface areas below 10 $\mu m^2\ cm^{-3}$. In remote regions, surface areas above 40 $\mu m^2\ cm^{-3}$ can be dominated by sea salt aerosol in the MBL but usually combustion aerosol aloft. Intermediate values of the RCN (0.2–0.6) ratio aloft often indicate contributions from both sources. Pollution plumes in the Tropics were generally confined below about 6 km. Major events such as the Asian dust and pollution transport mentioned here are about an order of magnitude larger than other more common continental plumes evident in the tropical data.

We note that the use of the RefRatio to stratify clean and continentally influenced air in Fig. 14 should not be interpreted as stratification of vertical profiles into clean and continentally influenced profiles per se. In practice, most profiles flown exhibit a layer structure with continentally influenced rivers of aerosol often separated by clean regions and vice versa. Rather, the profiles in Fig. 14 illustrate the relative perturbation of clean aerosol properties that have been observed as a result of continental aerosol influence at any altitude. This may be of use to modelers who wish to turn off continental particle sources and look and the roles of gas to particle conversion only in contributing to aerosol number, area, volume, or light scattering over the Pacific.

5. Conclusions

The Pacific free troposphere was shown to have aerosol predominately sourced from natural nucleation of aerosol from cloud outflow and from long-range transport of continental emissions. The natural source tends to dominate number concentrations aloft over most regions, but when continental aerosol is present it tends to dominate aerosol surface, mass, and light scattering. Nuclei formed in the Tropics appear to spread in the FT between about 20°S and 35°N, perhaps as a result of the Hadley circulation. Greater continental contributions to FT aerosol is evident in the Northern Hemisphere above 35°N. Convective process over the Southern Ocean also result in significant production of new aerosol but at lower altitudes due to lower temperature, making these new nuclei more readily brought in contact with the MBL than in the Tropics. Both clean and continental aerosol can subside and be entrained into MBL to alter the population of MBL aerosol including available CCN.

In this paper we have placed greater emphasis on new particle production and evolution and its relation to large-scale aerosol features in the troposphere. In a subsequent paper (Part II, in preparation) we will place greater emphasis on the total size distribution, its physiochemical properties, and links to aerosol optical properties including greater emphasis on continental sources.

Acknowledgments. Primary support for this analysis was provided under the NASA Global Aerosol Climatology Project (NAG5-8118) with additional resources provided under NASA (NCC-1-315) and Office of Naval Research (N00014-96-1-0320). We also thank Dr. Bruce Anderson for providing much of the high-altitude CN data obtained from the NASA DC-8 during the PEM-Tropics B programs, Rodney Weber for his ultrafine nuclei data near cloud edges, and Jim Spinhirne of GSFC for the lidar imagery from GLOBE.

REFERENCES

Bates, T. S., and Coauthors, 1998: Processes controlling the distribution of aerosol particles in the lower marine boundary layer during the First Aerosol Characterization Experiment (ACE-1). *J. Geophys. Res.,* **103,** 16 369–16 384.

Brechtel, F., S. Kreidenweis, and H. Swan, 1998: Air mass characteristics, aerosol particle number concentrations and number size distributions at Macquarie Island during ACE-1. *J. Geophys. Res.,* **103,** 16 351–16 367.

Charlson, R. J., J. E. Lovelock, M. O. Andreae, and S. G. Warren, 1987: Oceanic phytoplankton, atmospheric sulfur, cloud albedo and climate. *Science,* **326,** 655–661.

——, S. E. Schwartz, J. M. Hales, R. D. Cess, J. A. Coakley Jr., J. E. Hansen, and D. J. Hofmann, 1992: Climate forcing by anthropogenic aerosols. *Science,* **255,** 423–430.

Clarke, A. D., 1989: Aerosol light absorption by soot in remote environments. *Aerosol Sci. Technol.,* **10,** 161–171.

——, 1991: A thermo-optic technique for in-situ analysis of size-resolved aerosol physicochemistry. *Atmos. Environ.,* **25A,** 635–644.

——, 1993: A global survey of atmospheric nuclei in the remote midtroposphere: Their nature, concentration and evolution. *J. Geophys. Res.,* **98** (D11), 20 633–20 647.

——, and J. N. Porter, 1993: Pacific marine aerosol. Part II: Equatorial gradients, ammonium and chlorophyll during SAGA3. *J. Geophys. Res.,* **98** (D9), 16 997–17 010.

——, Z. Li, and M. Litchy, 1996: Aerosol dynamics in the Pacific marine boundary layer: Microphysics, diurnal cycles and entrainment. *Geophys. Res. Lett.,* **23,** 733–736.

——, T. Uehara, and J. Porter, 1997: Atmospheric nuclei and related aerosol fields over the Atlantic: Clean subsiding air and continental pollution during ASTEX. *J. Geophys. Res.,* **102** (D21), 25 821–25 292.

——, J. L. Varner, F. Eisele, R. Tanner, L. Mauldin, and M. Litchy, 1998: Particle production in the remote marine atmosphere: Cloud outflow and subsidence during ACE-1. *J. Geophys. Res.,* **103,** 16 397–16 409.

——, and Coauthors, 1999a: Nucleation in the equatorial free troposphere: Favorable environments during PEM-Tropics. *J. Geophys. Res.,* **104,** 5735–5744.

——, V. N. Kapustin, F. L. Eisele, R. J. Weber, and P. H. McMurry, 1999b: Particle production near marine clouds: Sulfuric acid and predictions from classical binary nucleation. *Geophys. Res. Lett.,* **26,** 2425–2428.

——, W. Collins, P. Rasch, V. Kapustin, K. Moore, and S. Howell, 2001: Dust and pollution transport on global scales: Aerosol measurements and model predictions. *J. Geophys. Res.,* in press.

Covert, D. S., V. N. Kapustin, T. S. Bates, and P. K. Quinn, 1996: Physical properties of marine boundary layer aerosol particles of the mid-Pacific in relation to sources and meteorological transport. *J. Geophys. Res.,* **101,** 6919–6930.

Cutten, D. R., R. F. Peuschel, D. A. Bowdle, V. Srivastava, A. D. Clarke, J. Rothermel, J. D. Spinhirne, and R. T. Menzies, 1996: Multiwavelength comparison of modeled and measured aerosol backscatter over Pacific Ocean. *J. Geophys. Res.,* **101** (D5), 9375–9389.

Duce, R. A., and N. W. Tindale, 1991: Atmospheric transport of iron and its deposition in the ocean. *Limnol. Oceanogr.,* **36,** 1715–1726.

Eisele, F. L., and D. J. Tanner, 1993: Measurement of the gas phase concentration of H_2SO_4 and methane sulfonic acid and estimates of H_2SO_4 production and loss in the atmosphere. *J. Geophys. Res.*, **98,** 9001–9010.

Fitzgerald, J. W., 1991: Marine aerosols: A review. *Atmos. Environ.*, **25A,** 533–545.

Heintzenberg, J., D. S. Covert, and R. Van Dingenen, 2000: Size distribution and chemical composition of marine aerosols: A compilation and review. *Tellus*, **52B,** 1104–1122.

Hoell, J., and Coauthors, 1999: Pacific Exploratory Mission in the Tropical Pacific: PEM-Tropics A, August–September 1996. *J. Geophys. Res.*, **104,** 5567–5584.

Hoppel, W. A., G. M. Frick, and R. E. Larson, 1986: Effect of nonprecipitating clouds on the aerosol size distribution in the marine boundary layer. *Geophys. Res. Lett.*, **13,** 125–128.

——, J. W. Fitzgerrald, G. M. Frick, R. E. Larson, and E. J. Mack, 1990: Aerosol size distributions and optical properties found in the marine boundary layer over the Atlantic Ocean. *J. Geophys. Res.*, **95,** 3659–3686.

Jaffe, D., and Coauthors, 1999: Transport of Asian air pollution to North America. *Geophys. Res. Lett.*, **26,** 711–714.

Jennings, S. G., and C. D. O'Dowd, 1990: Volatility of aerosols at Mace Head on the west coast of Ireland. *J. Geophys. Res.*, **95,** 13 937–13 948.

King, M. D., Y. J. Kaufman, D. Tanre, and T. Nakajima, 1999: Remote sensing of tropospheric aerosols from space: Past, present, and future. *Bull. Amer. Meteor. Soc.*, **80,** 2229–2259.

O'Dowd, C. D., M. H. Smith, I. E. Consterdine, and J. A. Lowe, 1997: Marine aerosol, sea-salt and the marine sulphur cycle: A short review. *Atmos. Environ.*, **31,** 73–80.

Quinn, P. K., S. F. Marshall, T. S. Bates, D. S. Covert, and V. N. Kapustin, 1995: Comparison of measured and calculated aerosol properties relevant to the direct radiative forcing of sulfate aerosols on climate. *J. Geophys. Res.*, **100,** 8977–8991.

——, V. N. Kapustin, T. S. Bates, and D. S. Covert, 1996: Chemical and optical properties of marine boundary layer aerosol particles of the mid-Pacific in relation to sources and meteorological transport. *J. Geophys. Res.*, **101,** 6931–6951.

Raes, F., 1995: Entrainment of free tropospheric aerosols as a regulating mechanism for cloud condensation nuclei in the remote marine boundary layer. *J. Geophys. Res.*, **100,** 2893–2903.

Sollazzo, M. J., L. M. Russel, D. Percival, S. Osborne, R. Wood, and D. W. Johnson, 2000: Entrainment rates during ACE-2 Lagrangian experiments calculated from aircraft measurements. *Tellus*, **52B,** 335–347.

Srivastava, V., A. D. Clarke, M. A. Jarzemski, J. Rothermel, D. R. Cutten, and D. A. Bowdle, 1997: Comparison of modeled backscatter using measured aerosol microphysics with focused CW lidar data over Pacific. *J. Geophys. Res.*, **102,** 16 605–16 618.

Stowe, L. L., A. M. Ignatov, and R. R. Singh, 1997: Development, validation, and potential enhancements to the second-generation operational aerosol product at the National Environmental Satellite, Data, and Information Service of the National Oceanic and Atmospheric Administration. *J. Geophys. Res.*, **102,** 16 889–16 910.

Wexler, A. S., F. W. Lurmann, and J. H. Seinfeld, 1994: Modeling urban and regional aerosols, 1, Model development. *Atmos. Environ.*, **28,** 531–546.